JOURNAL OF AIRCRAFT
Vol. 33, No. 5, September–October 1996

Aerodynamic Characteristics of Aircraft Under Side Gust

Ibrahim A. Olwi*
King Abdulaziz University, Jeddah 21413, Saudi Arabia

Wind-tunnel tests were conducted to investigate the aerodynamic characteristics of an aircraft when exposed to side gust resulting from microburst windshear. External airstream was supplied through the test section side wall such that it was normal to the flight pathline and parallel to the ground. The effect of side gust was studied in terms of the model performance in undisturbed flight compared to its response during side flow. The model aerodynamic characteristics were examined at several sideslip angles as well as during straight flight. The wind-tunnel results of the straight-flight mode indicated that as side gust was introduced, there was a slight but consistent drop in lift, considerable accumulation of drag, increase in nose-up pitching moment, and constant lateral drift. The loss of lift became more appreciable at negative sideslip angles. In remedy, this situation was associated with a minimal amount of added-on drag. It was demonstrated that such loss of lift could be minimized by yawing the aircraft in the opposite direction, i.e., as the gust direction became closer to being head wind. However, this configuration of positive sideslip yielded higher accumulation of drag. Severe nose-up pitching moment was experienced during side gust exposure at negative sideslip orientations. It is found that while the trim condition was displaced, the stability margin was retained unaffected.

Nomenclature

C_D = drag coefficient
C_L = lift coefficient
C_{MP} = pitching moment coefficient, taken about the wing mean aerodynamic quarter-chordline; considered positive for nose-up moment
C_{MR} = rolling moment coefficient, considered positive for downward starboard wing moment
C_S = side force coefficient, considered positive when forced towards the starboard wing
α = angle of attack, deg
β = sideslip angle, deg

Introduction

MICROBURST windshear is responsible for most aircraft accidents resulting from meteorological conditions.[1] The number of accidents related to low-level windshear (more than 40 in the last three decades), and the number of fatalities involved (more than 600), dictated a major research effort in the subject matter. The hazard of microburst windshear is most serious when it gets close to the ground, where it changes its direction from downflow to flow parallel to the ground in all directions. The main threat in such flow regions is the flow that is parallel to the aircraft flight path, i.e., the flow that is head/tail wind, where the aircraft is being exposed to a sudden increase in lift followed by a sudden and drastic loss of lift.

Tremendous effort was devoted to learn the causes and understand the flowfield associated with the low-level windshear phenomenon.[2,3] The means envisaged to understand the problem have included meteorological simulation models,[4,5] analysis of flight records for actual microburst windshear encounters,[6–8] the study of airplane design requirements in lieu of gust loads implications,[9] and wind-tunnel experiments to study the aircraft performance as it experiences windshear.[10–14] The most urgent quest was to develop warning systems that could detect severe microburst windshear regions to alert the flight crew during an aircraft's final approach for landing or takeoff.[15–19]

The main threat of low-level windshear is the sharp sudden change in speed and/or direction of airflow over the aircraft, which takes place when the aircraft flight path passes through the center of the microburst. Naturally, most of the past research work has focused on this particular situation, i.e., on longitudinal winds and the resulting longitudinal aircraft performance. It was concluded from those studies that if microburst windshear was detected, the pilot should be advised to avoid the dangerous core region.

The pilot, in such a case, may be able to divert the aircraft to a flight path that is off the microburst center. Henceforth, the aircraft would not experience the drastic loss of lift. Rather, it would be subject to a flowfield that has the same microburst speed, but is of lateral direction; defined as side gust. Though this situation complements the head/tail wind case, it has received much less research effort. As a matter of fact, one can hardly come across results of actual flight data or wind-tunnel experiments dealing with lateral side gust phenomenon.

The drive behind this work is to address the issue of safety in terms of the aerodynamic characteristics when side gust is encountered. This article looks into the matter of side gust contribution to the basic aerodynamic trends of an aircraft model at various angles of attack (AOAs). To achieve this objective, external flow is supplied to the wind tunnel through its test section side wall. The effect of side gust is examined by comparing the forces and moments experienced by the aircraft during undisturbed flight and while being exposed to external side flow. The investigation is carried out for several sideslip angles to identify the sideslip orientation that is most affected by side gust.

Experimental Model and Facility

The experimental facility included a low-speed wind tunnel, a fan-duct system to provide side gust through the tunnel test section side wall, an aircraft model, a data acquisition system, and a range of related manometers/transducers. The wind tunnel was a nonreturn blowdown type, with a test section 2 m long, 0.5 m high, and 0.7 m wide.

Side gust was simulated by blowing crossflow through an opening at the tunnel test section side wall. The opening di-

Presented as Paper 94-3496 at the AIAA Atmospheric Flight Mechanics Conference, Scottsdale, AZ, Aug. 1–3, 1994; received Oct. 18, 1995; revision received May 5, 1996; accepted for publication May 8, 1996.

*Associate Professor, Aeronautical Engineering Department, P.O. Box 9027. Senior Member AIAA.

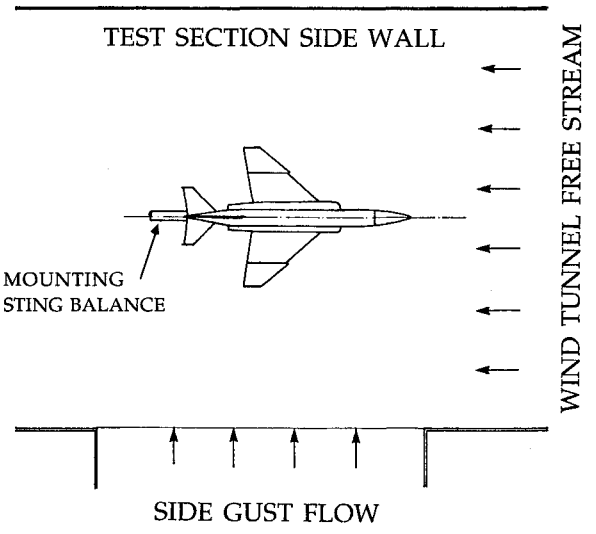

Fig. 1 Top view of the aircraft model placed in the wind-tunnel test section. Flow directions are indicated.

mensions were 0.54 m wide and 0.30 m high. The injected flow was provided through a settling chamber, in which uniform streamlined flow was attained. Three levels of screens were utilized to enhance flow uniformity. Two blowers were employed to supply the mass flow to the chamber through 0.2-m ducts. When operated while the tunnel was running, the blowers delivered crossflow to the tunnel at a speed of 8.2 m/s. The wind-tunnel freestream velocity, measured upstream of the model and the crossflow opening, was fixed at 20.5 m/s, i.e., 2.5 times the side flow. The airspeed was measured by a pitot tube connected to a digital micromanometer. The parameters of investigation were the AOA and the sideslip angle.

Military fighter aircraft are normally smaller than conventional passenger aircraft and, consequently, are more susceptible to be influenced by meteorological hazards. Therefore, the tests were carried out on a fighter aircraft model. The model used in the investigation was a replica of a scaled-down model of the McDonnell Douglas F-4 Phantom fighter aircraft. The overall model dimensions were 0.024-m tip chord, 0.120-m root chord, 0.072-m mean chord length, 0.240-m span, and 0.375-m fuselage length. The model was mounted on a strain gauge six-component sting balance to measure the forces and moments applied on the aircraft. The top view of the model and its position in the test section with respect to the opening for supplying side flow is illustrated in Fig. 1.

Results and Discussion

The wind tunnel was operated at a constant freestream velocity of 20.5 m/s corresponding to a Reynolds number of 1.04×10^5, based on the model mean aerodynamic chord length. Crossflow was supplied through the test section side wall at a rate of 8.2 m/s through a duct flow area of 0.162 m^2. The longitudinal and lateral components of forces and moments experienced by the aircraft model were measured during both undisturbed flight conditions and when the aircraft was subjected to side flow.

Study of the transient behavior of the aircraft model, from the onset of external side flow until the flow supplied reached a steady value, had not been part of the experimental program. Rather, side gust effects were examined via comparing the model aerodynamic characteristics during undisturbed flight to the case when the aircraft was under steady external lateral flow. The experiments were conducted under a fixed tunnel flow and at a given model orientation setting. The model was tested at AOAs ranging from 0 to 20 deg at steps of 2 deg. The investigation incorporated the aircraft performance at sideslip variations from −10 to 10 deg at steps of 5 deg. The direction of sideslip was considered positive when the starboard wing led the port wing.

Measurements During Straight Flight

The first set of results is presented in Fig. 2 when the aircraft is at a zero sideslip angle as defined in Fig. 1. Figure 2a displays the variation of C_L vs α. For the case of no gust, the lift curve is linear up to 16-deg AOA before starting to stall. It is also observed that the lift–curve slope is not affected with the introduction of crossflow, but stall is delayed such that the linear part of the $C_L-\alpha$ curve is extended to 18 deg. It is recognized from the figure that even though the intensity of side flow is relatively appreciable, equivalent to 0.4 times the freestream, the drop in the lift force is mild and does not pose a substantial threat. Quantitatively, the net drop in lift was 0.89 (on the average for $0 \leq \alpha \leq 16$ deg) corresponding to about a 16% reduction from the original lifting force. This is quite different from the performance loss resulting from the downward flow of a microburst windshear, covered in Refs. 10–13, when the gust direction is head/tail wind. In that case and during straight flight, the loss of lift is quite significant. For example, the results obtained by Olwi et al.,[10] taken at the same tunnel freestream and an equivalent external flow speed to the present study, yielded an average drop in C_L of 0.57 (but for the range of $0 \leq \alpha \leq 12$ deg) representing 34% lift depletion because of microburst windshear encounter. It must be noted, however, that the model used in Ref. 10 was of a generic transport aircraft.

The drag polars, C_D-C_L curves presented in Fig. 2b, demonstrate that the drag force is increased as the aircraft is exposed to side flow. This is in line with the previous results obtained during windshear exposure.[10–14,20] It is evident from

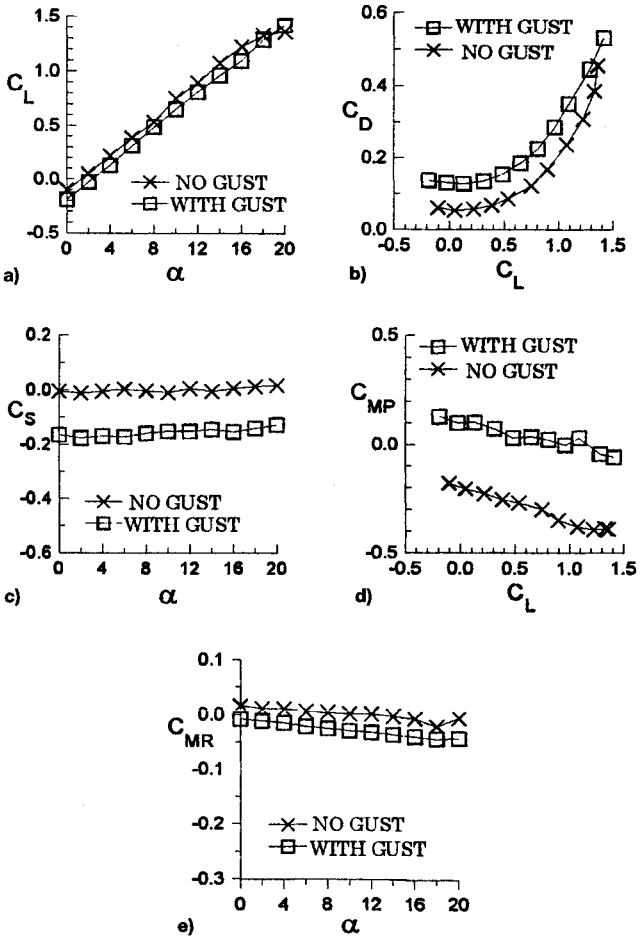

Fig. 2 Aerodynamic characteristics of the model when subjected to side gust, during straight flight.

the figure that the effect of side gust on the drag force is dependent on the AOA. The effect on C_D is more pronounced at low values of C_L, i.e., when the AOA is small. As high angles are attained, the increase in drag diminishes. This leads one to conclude that if the aircraft is being exposed to side gust loads during straight flight at low angles of attack, it is recommended to increase the angle of attack such that the increase in drag is minimal and, naturally, more lift is obtained.

Figure 2c illustrates C_S when the model is exposed to cross-flow as a function of the AOA. It must be stated that this external flow is supplied to the tunnel from the starboard wing side, i.e., in the direction of negative side force. As anticipated, when there is no external flow, the aircraft does not experience side forces if it is in straight flight. The consequence of blowing side wind is to push the aircraft in the wind direction, resulting in appreciable negative side forces. The figure demonstrates that this side drift is independent of the AOA, as will be discussed later when the plots in Fig. 5 are examined.

In Fig. 2d C_{MP} is plotted against the lift coefficient. It is demonstrated that encountering side flow has no influence on the stability margin and, hence, the aircraft attains a stable flight. However, the gust displaces the equilibrium condition, the trim, towards other lift values. This may be attributed to the overriding crosswind exposure resulting in a constant increase of the pitching moment.

Figure 2e elucidates C_{MR}. It is noticed that the introduction of side flow adds negative rolling moment on the aircraft model during straight flight. This indicates that the aircraft under side gust tends to roll about the longitudinal angle with a negative bank angle such that the starboard wing becomes higher than the port wing.

Effects of Sideslip

Each figure in this section depicts the model aerodynamic characteristics at sideslip angles of 5, 10, −5, and −10 deg, respectively, with each figure being dedicated to only one force/moment.

Figure 3 demonstrates that the resulting drop in lift is mild, especially at high AOAs. It is noticed, however, that when the aircraft is in level flight ($\alpha = 0$ deg) or at very low AOAs, the lifting force vanishes and only downward force could be obtained as depicted in the four cases of Fig. 3. As the aircraft model is set at the negative sideslip orientation of $\beta = -10$ deg, the slope of the C_L–α curve gets slightly increased, the zero-lift AOA increases, and the amount of lift lost because of side gust exposure is found to reach appreciable values, as depicted in Fig. 3d. To quantify the latter observation, Table 1 is presented.

Table 1 is constituted of two groups of data; the first one encompasses the lift coefficients taken at low AOAs ($0 \leq \alpha < 10$ deg), and the values in the second group are obtained at high AOAs ($10 < \alpha \leq 20$ deg). The first row of data in each group (sets 1a and 2a) represents the readings of C_L taken during undisturbed flight, i.e., no gust, whereas the lift coefficient values measured while side flow is supplied constitute the data of the second row in each group (sets 1b and 2b). The third row (sets 1c and 2c) is the average drop in the lift coefficient because of side flow, i.e., the difference between the first two rows. The last row (sets 1d and 2d) is the same as the third row, but is given in percentage form. The data columns of the table refer to Figs. 3a–3d, respectively.

It is evident from the data in this table that the contribution of side gust on the lift coefficient is appreciable when the aircraft is flying at low AOAs. Though the net drop in C_L might not be large in some sideslip orientations (compare sets 1c and 2c), the relative effect poses a threat (compare sets 1d and 2d), because the original values of C_L are small; resulting in a relative value of at least 50% (refer to data set 1d). In particular, the amount of lift lost at $\beta = -10$ deg is quite high; both as net value ($\Delta C_L = 0.325$) and in relative value (94%) as well.

Table 1 Average values of the lift coefficient for low and high ranges of the AOA and for several sideslip angles

	β, deg			
Set	5	10	−5	−10
	Low angles of attack ($0 \leq \alpha < 10$ deg)			
1a	0.3372	0.3030	0.3417	0.3450
1b	0.1399	0.1281	0.1179	0.0199
1c	0.1973	0.1749	0.2237	0.3251
1d	59%	58%	65%	94%
	High angles of attack ($10 < \alpha \leq 20$ deg)			
2a	1.1800	1.1644	1.1998	1.1630
2b	1.0859	1.0217	1.0456	1.0252
2c	0.0941	0.1427	0.1542	0.1378
2d	8%	12%	13%	12%

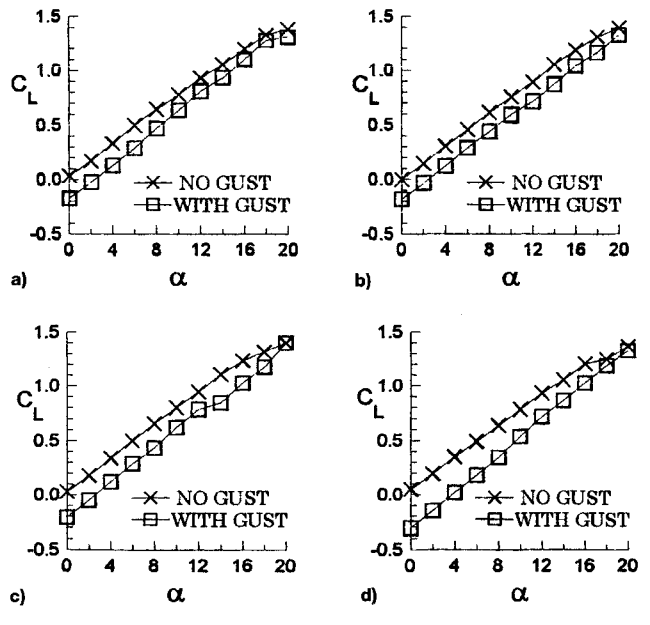

Fig. 3 Effect of side gust on the lift coefficient for the following sideslip angles: β = a) 5, b) 10, c) −5, and d) −10 deg.

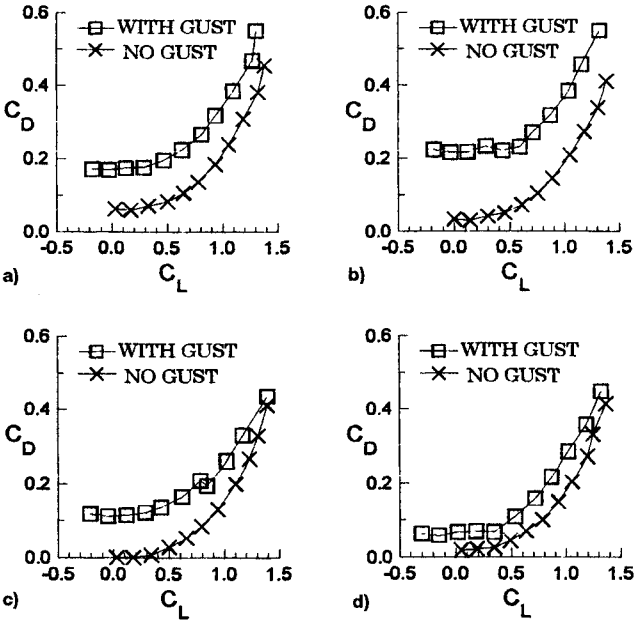

Fig. 4 Effect of side gust on the drag polars for the following sideslip angles: β = a) 5, b) 10, c) −5, and d) −10 deg.

The drag polar diagrams are displayed in Fig. 4. It is found that, as side flow is introduced, the maximum increase in C_D occurs generally at low α, and the minimum added-on drag is attained at high angles of attack. This is in line with the observation made earlier about the drag polars of Fig. 2b. It appears that when the model nose is closest to the external flow opening, i.e., at negative sideslip, the effect of side gust on the drag force is minimized (Fig. 4d). On the other hand, the most considerable increase in the drag force is suffered at 10-deg sideslip (Fig. 4b). At this setting, the average increase in the drag coefficient is $\Delta C_D = 0.1468$ (representing a relative increase of about 95%), whereas the corresponding values at -10-deg sideslip orientation are 0.0226 and 15%, respectively.

The effect of side gust is quite consistent on the side force for all sideslip angles, as demonstrated in Fig. 5. When there is no side flow, positive sideslip orientations would naturally create negative side force, and the opposite would be experienced at negative sideslip. As the model is subjected to external flow from the starboard wing, the model is pushed in the direction of the flow, i.e., resulting in negative side force. This drift experienced by the aircraft could exceed the side force resulting from sideslip alone, as depicted in Figs. 5a and 5b. The contribution of such flow could be strong enough to override the side forces arising from sideslip at negative yaw angles (Figs. 5c and 5d), such that the aircraft would be forced back to drift in the direction of the lateral flow.

To verify the net drift caused by side gust, Table 2 is provided. It outlines the difference in the values of the side force applied on the aircraft model caused by introducing side flow in the tunnel. The response is shown for only four representative AOAs against all sideslip angles covered in the tests. The increase in the resulting side force is almost constant during level flight ($\alpha = 0$ deg) except for slightly higher drift at 10-deg sideslip. For all other AOAs, the same trend is attained, but with much stronger drift at that orientation. This observation emphasizes the importance of knowing the aircraft sensitivity in terms of the aerodynamic characteristics to some sideslip angles relative to the gust direction.

Therefore, Table 3 is presented to explore the relative contribution of this drift on the aircraft performance compared with that during calm flight without gust loads. The values in this table represent the percent increase in side force, caused from external flow, divided by its value measured before applying such a flow. The main feature in this table is the relative change in side force experienced by the aircraft during straight flight as side flow is applied. These values are so high because at this setting the aircraft would essentially be under no lateral effects. Then, as it flies through the side gust zone, it will suddenly be exposed to a side force, resulting in abrupt strong lateral drift, a fact that the flight crew should be aware of. This is found to be most severe at low AOAs. Fortunately, the aircraft usually flies at high AOAs during takeoff and landing, the region where side gust could pose serious impact on the aircraft performance.

The stability curves are demonstrated in Fig. 6 for various sideslip angles. It is indicated that a strong nose-up pitching moment is the overriding phenomenon caused by side gust exposure. This parasite pitching moment does not alter the stability margin but, on the other hand, changes the trim condition. It appears that this overriding pitching moment is approximately constant for positive sideslip angles (Figs. 6a and 6b). However, it increases as the sideslip angle takes on negative values, as depicted in Figs. 6c and 6d.

The contribution of side wind on the rolling moment at different sideslip angles is provided in Fig. 7. It seems that cross-

Table 2 Values of the net side drift experienced in response to gust loads for a selected sample of AOAs

	β, deg				
α, deg	−10	−5	0	5	10
0	−0.156	−0.171	−0.161	−0.165	−0.186
6	−0.167	−0.166	−0.175	−0.155	−0.246
12	−0.181	−0.177	−0.159	−0.146	−0.247
20	−0.163	−0.143	−0.145	−0.161	−0.266

Table 3 Relative values of the side drift experienced in response to gust loads for a selected sample of AOAs[a]

	β, deg				
α, deg	−10	−5	0	5	10
0	−0.86	−1.90	42.39	1.42	0.93
6	−0.89	−1.84	−49.97	1.58	1.33
12	−0.91	−2.04	−22.41	1.39	1.34
20	−0.83	−1.81	−8.23	1.95	1.60

[a]Values given are percent.

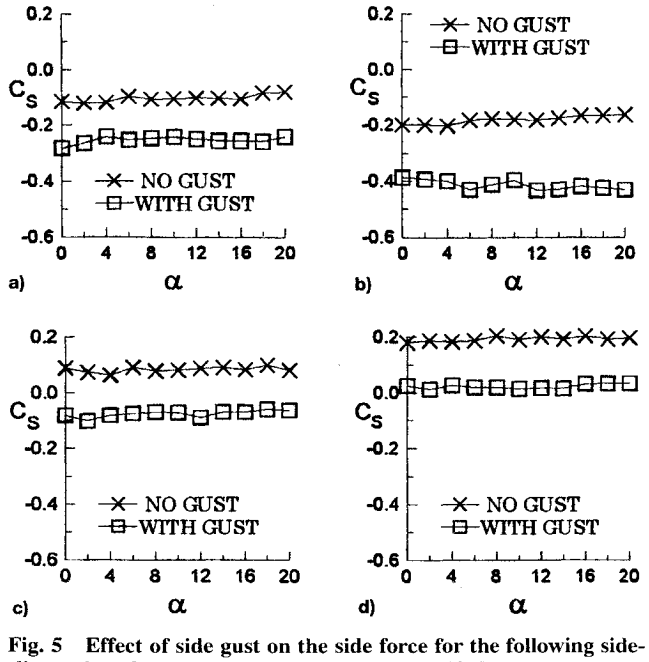

Fig. 5 Effect of side gust on the side force for the following sideslip angles: β = a) 5, b) 10, c) −5, and d) −10 deg.

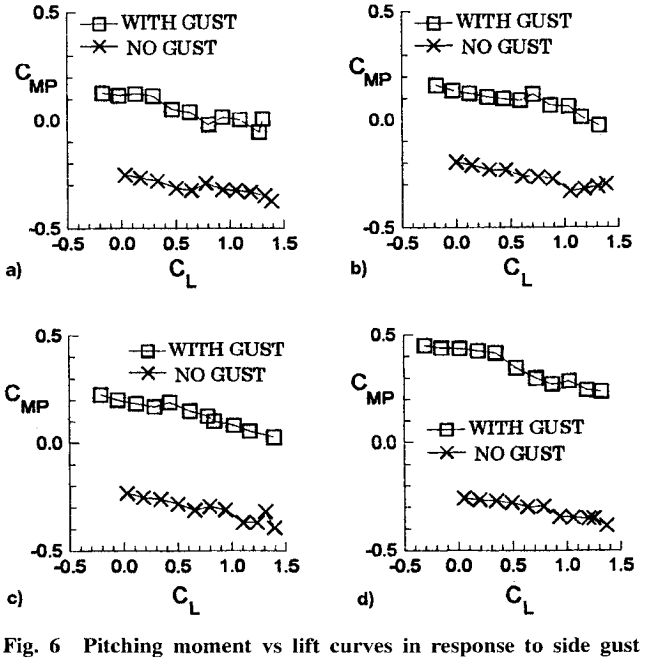

Fig. 6 Pitching moment vs lift curves in response to side gust loads for the following sideslip angles: β = a) 5, b) 10, c) −5, and d) −10 deg.

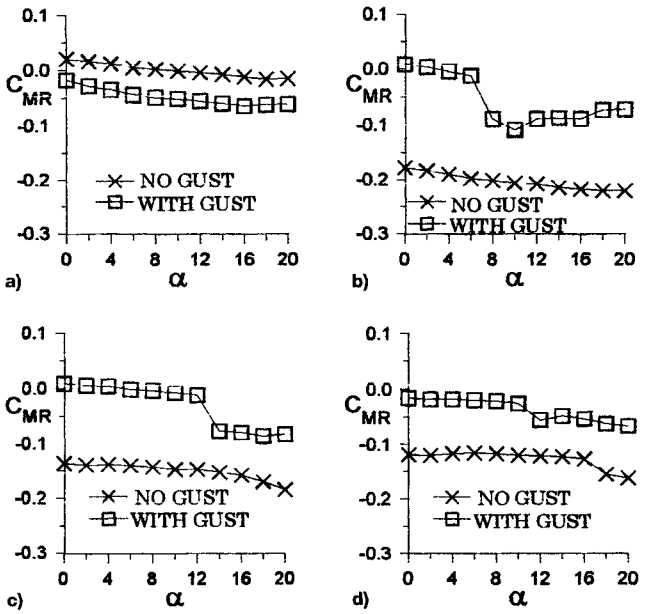

Fig. 7 Effect of side gust on the rolling moment for the following sideslip angles: β = a) 5, b) 10, c) −5, and d) −10 deg.

flow tends to add a positive rolling moment. Since there are no control elements employed in the tests, this overriding rolling moment is a consequence of reducing the lift on the starboard wing that faces side gust.

Conclusions

An array of experiments was conducted to investigate the effect of side gust on an aircraft model. The tests were conducted in a low-speed wind tunnel in which crossflow was supplied through the test section side wall. The aircraft response was examined through measurements of the aerodynamic forces and moments. During straight flight, the change in the lift characteristics was mild: a slight loss of lift and delay of stall. However, there was a significant increase in drag, especially at low AOAs. The stability margin was not affected, in this orientation, but the equilibrium condition was displaced. As for the lateral force, there was a strong tendency to drift the aircraft in the gust direction. With the introduction of side gust, the aircraft experienced negative rolling moment.

Results at several sideslip angles indicated that the impact of side gust on the aircraft performance varied according to the aircraft orientation angles. Specifically, there was a substantial increase in drag at positive sideslip angles, particularly at low AOAs. The results showed that this added-on drag, resulting from side flow, could be minimized by yawing the aircraft to negative sideslip settings. The reduction in lift was not appreciable in general, but started to increase by yawing the aircraft towards more negative sideslip settings especially at low AOAs. The side force experienced by the aircraft when encountering side flow, at a given sideslip setting, was almost constant. This side drift got stronger as the aircraft was yawed clockwise to be in a position of higher headwind, i.e., at positive sideslip configuration. A strong nose-up pitching moment was dominant because of gust exposure. In particular, drastic nose-up pitching moment was recorded at high negative sideslip settings. While the trim condition was displaced, because of side gust, the stability margin was unaffected.

References

[1]Al-Bahi, A., Ghazi, M., Olwi, I., and Aly, M., "The Effect of Downcoming Burst on the Pressure Distribution of Wing Sections," *Proceedings of the 4th International Conference of Fluid Mechanics (ICFM4)* (Cairo, Egypt), College of Engineering, Alexandria Univ., Alexandria, Egypt, 1992, pp. 359–368.

[2]Federal Aviation Administration, "Low Level Wind Shears," *Advisory Circular*, AC 00-50A, 1979.

[3]Hoblit, F. M., *Gust Loads on Aircraft: Concepts and Applications*, AIAA Education Series, AIAA, Washington, DC, 1989.

[4]Fleeter, S., Capece, V. R., and Chiang, H. D., "Unsteady Aerodynamic Gust Response Including Steady Flow Separation," *AIAA Journal*, Vol. 28, No. 6, 1990, pp. 1024–1031.

[5]Jones, J. G., "Statistical Discrete Gust Theory for Aircraft Loads," *Royal Aircraft Establishment*, TR 73167, Farnborough, Hampshire, England, UK, 1983.

[6]Grantham, W. J., Roetcisoender, G. G., and Parks, E. K., "DFW Microburst Model Based on AA-539 Data," *Journal of Aircraft*, Vol. 27, No. 11, 1990, pp. 917–922.

[7]Schultz, T. A., "Multiple Vortex Ring Model of the DFW Microburst," *Journal of Aircraft*, Vol. 27, No. 2, 1990, pp. 163–168.

[8]Coppenbarger, R. A., and Wingrove, R. C., "Wind Measurements from Four Airliners in 1988 Denver Microburst," *Journal of Aircraft*, Vol. 27, No. 11, 1990, pp. 923–928.

[9]Fuller, J. R., "Evolution of Airplane Gust Loads Design Requirements," *Journal of Aircraft*, Vol. 32, No. 2, 1995, pp. 235–246.

[10]Olwi, I., Aly, M., Ghazi, M., and Al-Bahi, A., "A Study of Aerodynamic Forces and Pitching Moment on an Aircraft Model Subject to Wind Shear," *Proceedings of the 3rd Engineering Saudi Conference* (Riyadh, Saudi Arabia), College of Engineering, King Saud Univ., Riyadh, Saudi Arabia, 1991, pp. 438–442.

[11]Aly, M., Olwi, I., Al-Bahi, A., and Ghazi, M., "Experimental Investigation of the Wind Shear Effect on the Aerodynamic Forces on a Wing," AIAA Paper 91-3216, Sept. 1991.

[12]Ghazi, M., Al-Bahi, A., Aly, M., and Olwi, I., "Aerodynamic Performance of Wing Sections Subject to Microburst," 1st Pacific International Conf. on Aerospace Science and Technology (PICAST1), Tainan, Taiwan, ROC, Dec. 1993.

[13]Ghazi, M., Al-Bahi, A., Aly, M., and Olwi, I., "Aircraft Performance Under Downcoming Burst Hazard," *Proceedings of the 5th ASAT Conference*, Military Technical College, Cairo, Egypt, 1993.

[14]Abdel-Rahman, M., Ghazi, M., Olwi, I., and Al-Bahi, A., "Aircraft Spoiler Effects Under Wind Shear," *Journal of Aircraft*, Vol. 31, No. 1, 1994, pp. 154–160.

[15]McCarthy, J., Blick, E. F., and Elmore, K. L., "Airport Wind Detection and Warning System Using Doppler Radar: A Feasibility Study," *MCS, Inc.*, Boulder, CO, 1981.

[16]Kessler, E., "Low-Level Windshear Alert Systems and Doppler Radar in Aircraft Terminal Operations," *Journal of Aircraft*, Vol. 27, No. 5, 1990, pp. 423–428.

[17]Goff, R. C., and Gramzow, R. H., "The Federal Aviation Administration's Low Level Windshear Alert System: A Project Management Perspective," *Proceedings of the 3rd International Conference of the Aviation Weather System*, American Meteorological Society, Boston, MA, 1989, pp. 408–413.

[18]Kessler, E., "Use, Non-Use, and Abuse of Weather Radar," *Journal of Aircraft*, Vol. 25, No. 5, 1988, pp. 448–452.

[19]Bracalente, E. M., Britt, C. L., and Jones, W. R., "Airborne Doppler Radar Detection of Low-Altitude Wind Shear," *Journal of Aircraft*, Vol. 27, No. 2, 1990, pp. 151–157.

[20]Zhao, Y., and Bryson, A. E., "Aircraft Control in a Downburst on Takeoff and Landing," *Proceedings of the 29th IEEE Conference on Decision and Control*, Vol. 2, Inst. of Electrical and Electronics Engineers, New York, 1990, pp. 753–757.